

NASA-TM-107052 19960002903

NASA Technical Memorandum 107052

NSTAR Ion Thruster Plume Impacts Assessments

Roger M. Myers
NYMA, Inc.
Brook Park, Ohio

Eric J. Pencil and Vincent K. Rawlin
Lewis Research Center
Cleveland, Ohio

Michael Kussmaul
NYMA, Inc.
Brook Park, Ohio

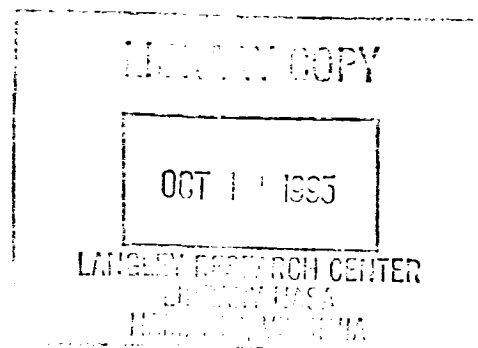
and

Katessha Oden
Tennessee State University
Nashville, Tennessee

Prepared for the
31st Joint Propulsion Conference and Exhibit
cosponsored by AIAA, ASME, SAE, ASEE
San Diego, California, July 10–12, 1995



National Aeronautics and
Space Administration





NSTAR ION THRUSTER PLUME IMPACTS ASSESSMENTS

Roger M. Myers
Nyma Inc., NASA Lewis Research Center
Brook Park, OH 44142

Eric J. Pencil and Vincent K. Rawlin
NASA Lewis Research Center
Cleveland, OH 44135

Michael Kussmaul
Nyma Inc., NASA Lewis Research Center
Brookpark, OH 44142

and

Katessha Oden
Tennessee State University
Nashville, TN 37209

Abstract

Tests were performed to establish 30-cm ion thruster plume impacts, including plume characterizations via near and far-field ion current measurements, contamination, and sputtering assessments. Current density measurements show that 95% of the beam was enclosed within a 22° half-angle and that the thrust vector shifted by less than 0.3° during throttling from 2.3 to 0.5 kW. The beam flatness parameter was found to be 0.47, and the ratio of doubly charged to singly charged ion current density decreased from 15% at 2.3 kW to 5% at 0.5kW. Quartz sample erosion measurements showed that the samples eroded at a rate of between 11 and 13 $\mu\text{m}/\text{hr}$ at 25° from the thruster axis, and that the rate dropped by a factor of four at 40° . Good agreement was obtained between extrapolated current densities and those calculated from tantalum target erosion measurements. Quartz crystal microbalance and witness plate measurements showed that ion beam sputtering of the tank resulted in a facility material backflux rate of $\sim 10 \text{ \AA}/\text{hr}$ in a large space simulation chamber.

Nomenclature

J_{tot}	Total ion beam current, A
R	Radius in beam, m
\bar{x}	x coordinate of beam center-of-pressure
\bar{y}	y coordinate of beam center-of-pressure
θ	probe rake angle

data available for 30-cm xenon thrusters operated at the NSTAR power levels of between 0.5 and 2.3 kW. This paper reports on preliminary measurements of NSTAR ion thruster plume properties and impacts performed to demonstrate diagnostics to be used in the final thruster integration assessments.

Introduction

The objective of the NASA Solar Electric Propulsion Technology Applications Readiness (NSTAR) program is to flight-qualify and demonstrate a 30-cm diameter xenon ion thruster system for primary propulsion applications.¹ In addition to thruster performance and lifetime demonstrations, satisfying the program objectives requires a complete assessment of the thruster plume impacts on spacecraft subsystems and functions. Potential plume impacts include sputtering, contaminant deposition, surface charging and discharging, and communications signal degradation. While ion thrusters have been the subject of extensive ground and space testing, there are currently no plume

Previous studies of ion thruster plume impacts have focussed on either thrusters using mercury propellant or low power, small diameter xenon thrusters. Byers,² reviewing results for mercury propellant thrusters, separates ion thruster plume impacts into those arising from the ion beam, low-energy plasma resulting from charge exchange collisions, neutral propellant, and non-propellant effluxes. While neutral mercury deposition can be quite deleterious to spacecraft surfaces, neutral xenon has no such effects and so is not directly considered in this study. Other studies have demonstrated diagnostics for the beam current density,³⁻⁵ doubly to singly charged current density ratio,⁶ and charge-exchange phenomena,^{6,7} all of which are required to establish plume divergence and impacts. Results of these studies have been used

to establish spacecraft integration requirements.^{8,9} For instance, once the ion beam is characterized, "exclusion zones" can be established to prevent sputtering of spacecraft surfaces. The doubly charged ion density impacts internal thruster erosion, thrust loss factors,¹⁰ and directly affects spacecraft integration because the ions are accelerated to twice the energy of the singly charged ions, and so can do greater damage than the singly charged ions. An understanding of the relationship between thruster operating parameters and the doubly to singly charged ion current ratio is necessary to ensure that the thruster is not operated at unreasonable conditions. Ion beam parameters are also used to establish thruster loss mechanisms.¹⁰

This paper reports on the development of beam diagnostics and preliminary results of ion beam diagnostics for the NSTAR 30-cm ion thruster. Following a brief description of the thrusters, facilities, and diagnostics, the results of beam current density measurements, doubly to singly charged ion current densities, sputtering, and contamination measurements are presented. The impact of the test facility on the measurements is also discussed. Finally, a summary of the major conclusions is given.

Thrusters and Vacuum Facilities

Two thrusters, a Functional Model (FMT) and an Engineering Model (EMT) thruster were used to measure the plume properties. A schematic of the EMT is shown in Fig. 1. Differences between the FMT and EMT are minor, and include an increase in accelerator grid thickness from 0.38 to 0.51 mm and a decrease in the grid compensation from 0.3% to 0.2%. Other changes are described in Ref. 11.

Tests were conducted in two vacuum facilities. The far-field ion current density and beam/surface impacts were measured in NASA's large space propulsion test bed, a 4.6-m diameter, 18-m long tank with 22 0.8-m diameter oil diffusion pumps and 27 m² of 20 K gaseous helium cryopumping surface.¹² The facility pressure with the NSTAR thruster operating at 2.3 kW and 0.5 kW were 1.9×10^{-4} Pa and 1.0×10^{-4} Pa, respectively. These pressures, and all those reported below, use an ion pressure gauge correction factor of 2.87 to adjust for the differential sensitivity of the gauges to air and xenon. The near-field ion current density and doubly-to-singly charged ion current ratios were measured in a smaller facility, a 1.5-m diameter, 4.3-m long tank with four 0.8-m diameter oil diffusion pumps. The facility pressures in this tank with the NSTAR thruster operating at

2.3 and 0.5 kW were 2.5×10^{-3} Pa and 8×10^{-6} torr, respectively.

Diagnostics and Experimental Configurations

Ion Current Density

Near-field ion current measurements were made using a 1-cm² area molybdenum probe rotated across the EMT centerline 2-cm downstream of the thruster on centerline. Because of the dished grids, this distance increased to 4.3-cm at the outer edge of the grids. The probe was biased to -34.2 V with respect to the tank ground and the probe current was measured using a 1-kohm shunt. All near-field measurements were made in the smaller vacuum facility, and should not have been affected by the higher facility pressure as the minimum charge-exchange mean-free path is 4-m at the highest facility pressure. This mean-free path was evaluated using the cross-sections given in Ref. 13.

Far-field ion current density measurements were made by rotating a 1.4-m-radius rake of eight Faraday probes located 3-m from the thruster exit plane through the plume. Far-field ion current measurements were made every 0.25 degrees as the probe rotated 365 degrees. The small overlap (5 degrees) was used to ensure full circumferential coverage. A similar technique has been described before.⁵ The eight Faraday probes were separated by 0.2 m and each probe consisted of a 0.5-inch diameter molybdenum disc with a 0.3-cm wide molybdenum guard ring separated from the main probe by a gap of 0.05-cm. Both the probes and guard rings were biased to -9.5 V with respect to tank ground for the measurements, and testing revealed that the results were insensitive to negative bias potential. The far-field measurements were made using the FMT in the large vacuum facility. The high pumping speed of this facility was required because the thruster/probe separation could result in substantial impacts from charge-exchange collisions. The charge-exchange mean-free-path ranged from ~60-m to ~80-m for pressures between 1.3×10^{-4} and 1.1×10^{-4} Pa.

Doubly to Singly Charged Ion Density Ratio

An ExB probe, fabricated at the Jet Propulsion Laboratory, was used to measure the relative concentration of doubly to singly charged ions in the EMT plume. The probe consisted of a 9.5-cm long collimator with 1.7-cm high, 0.10-cm wide slits at either end, a 14-cm long drift region, and a tungsten coated current collector located at the rear of the probe. Two permanent magnets and two bias electrodes oriented perpendicularly to provide the

crossed electric and magnetic fields required to separate the ion charge states. The two ion charge states are sampled by varying the bias voltage on the electrodes and measuring the current arriving at the collector. The probe geometry yields vertical and horizontal acceptance angles of 4.5 and 0.6 degrees, respectively. These measurements were made in the small vacuum facility using the EMT, and the ExB probe was mounted on a motor driven actuator which moved the probe vertically 140 cm from the thruster exit plane. The collimator and thruster were aligned horizontally for these measurements. In this configuration, the probe samples an area of the thruster which is 22-cm high and 2.9 cm wide, so that only gross non-uniformities would be detectable. No effort was made to point the collimator along the line-of-sight to the thruster when the probe was moved radially. For each operating condition, measurements of the doubles/singles ratio were first made on centerline to establish the bias voltages for the two ion population peaks. An example of this measurement is shown in Fig. 2, which shows that the doubles-to-singles current ratio with the EMT thruster operating at 2.3 kW is ~ 15% on centerline. Once the peak-signal bias voltages were established, the ExB probe was moved vertically across the ion thruster beam at each of the peak bias voltages to obtain the radial distribution of each ion charge state. The doubles to singles ratio was computed from these data.

Erosion and Contamination

An array of 24 diagnostic probes were used to evaluate the erosion and contamination potential of the NSTAR thruster and impacts of the vacuum facility. The probes consisted of polished quartz slides, tantalum samples, and two quartz-crystal microbalances (QCMs). The probe locations are shown in Fig. 3. All measurements were made during the two segments of the 2000 hr wear test described by Patterson,¹⁴ the first was 867 hr long and the second was 1163 hr long. For this test the thruster was mounted at an 8 degree angle to the facility centerline in the horizontal plane, and pointed 2 degrees upward.

Twelve polished quartz slides were placed along the walls of the tank to provide a profile of the net erosion and deposition throughout the tank. Additionally, three collimators, pointed at the thruster, were used with polished quartz samples to establish the thruster impacts independent of the tank material deposition. One of these collimators had a motorized shutter which was closed after 250 hrs in the first test segment and after 600 hrs in the second test segment in order to obtain a first-order measure of the erosion time dependence. The collimator design is describe in Ref. 15. The quartz samples were replaced after the first segment, providing a total of

four exposure durations for the collimated quartz slides. The four 7.6-cm square tantalum targets were placed 9.4 m axially from the thruster exit plane and arranged to measure the sputtering potential of the ion beam across the middle 2-m of the beam. The two QCMs and three witness plates were placed immediately beneath the NSTAR thruster to measure the backflux of tank material to the thruster. While these data are clearly not relevant to spacecraft integration assessments, they serve to quantify the effect of the ion beam in a ground test facility and to establish the effects, if any, of the facility on the ground-based thruster testing.

Results

Ion Current Density

Results for the near-field ion current density distribution are shown in Fig. 4. Measurements are shown for a thruster power of 2.3 kW at both the beginning and end of a 100 hr test with the screen grid tied to cathode common and with it floating. As can be seen from the plot, no changes were observed for any of the conditions. The beam flatness parameter, defined as the average beam current density divided by the peak beam current density, calculated from these results for the EMT is 0.47. This value is similar to that measured on other ion thrusters of similar design.¹⁶

Typical far-field ion current density measurements are shown in Fig. 5 for the FMT operating at power levels of 2.3, 1.5, and 0.5 kW. The discontinuity in the current density contour plots is an artifact of the probe motion control. The peak current density on beam centerline drops from 1.8 A/m² at the 2.3 kW setpoint to 0.7 A/m² at the 0.5 kW set point. Note that the centerline beam current density does not decrease in proportion to the thruster power level. To validate the far-field measurement, the two-dimensional current density profile was numerically integrated and compared with the actual beam current reduced by the calculated charge exchange fraction. The results are given in Table 1, and show that the agreement between the actual beam current and that obtained by integrating the probe measurements was within 10 % for cases in which charge exchange was below 10%. The current calculated from the probe measurements was always greater than expected. Increasing the facility pressure reduced the ion current measured at the probe location by increasing the number of charge exchange collisions in the beam. An example of this is given in Fig. 6, which shows the beam profile measured at a facility pressure of 1.2x10⁻³ Pa. This is a factor of nine higher than the lowest pressure achievable at this operating condition. The peak centerline current density decreased from 1.8 to 1.4 A/m², and the measured integrated current

(Table 1) decreased to 1.39 A, compared to the actual beam current of 1.72 A. Once again, the charge-exchange correction appears to be too large.

The two dimensional beam measurements were also used to calculate the enclosed current fraction as a function of angle from thruster centerline and the beam center-of-pressure. The former is required to assess both thrust loss due to beam divergence and to identify exclusion zones for placement of spacecraft surfaces, the latter is used to establish the degree of thrust vector misalignment and motion during throttling. Figure 7 shows the results of using a numerical integration routine to calculate the current enclosed as a function of angle from thruster centerline. The results show that over 80% of the beam was enclosed within a 15° half-angle for all power levels, and 95% was within 22°. The center-of-pressure coordinates for the beam were calculated from

$$\bar{x} = \frac{\sum_i \sum_N R_{ij} j(R_i, \theta_N) \cos \theta_N \Delta r \Delta \theta}{J_{\text{tot}}}$$

$$\bar{y} = \frac{\sum_i \sum_N R_{ij} j(R_i, \theta_N) \sin \theta_N \Delta r \Delta \theta}{J_{\text{tot}}}$$

where the first sum is over the probe radii and the second is over the measurement angle. The result can then be converted to an angle using the known distance between the thruster and the probe rake. Results for the FMT operating at 2.5, 1.5, and 0.5 kW show thrust vector angles of 0.44, 0.28, and 0.16 degrees, respectively. These results indicate that the misalignments in thrust vector were small and exhibit little shift while throttling the thruster.

Doubly to Singly Charged Ion Density Ratio

The radial distribution of the doubly to singly charged ion current density ratio is shown in Fig. 8 for three NSTAR thruster power levels with the EMT screen grid tied to cathode common. The doubles to singles ratio was approximately constant across the thruster (radius of 15 cm), and is ~ 15%, 10%, and 4% for the 2.3, 1.5, and 0.5 kW operating condition. When the screen grid was floated the doubles to singles ratio increased by about five absolute percentage points, and reducing the main flow by 6% while maintaining the beam current at 1.77 A increased the ratio to ~ 24%. Note that the uniformity of the measured distribution across the thruster is likely an artifact of the large probe sampling area discussed above, and can only be used to show that there are no major non-uniformities in the beam.

Erosion and Contamination

Results from the twelve uncollimated quartz slides mounted on the sides of the large vacuum facility showed that for included angles from the EMT thruster centerline smaller than 40° the slides were subjected to net erosion. For larger included angles the slides on both sides of the tank were in regions of net deposition from tank wall material. The three collimated quartz slides, two located at an angle of 25° for thruster centerline and one located at 40° (Fig. 2), all suffered net erosion. The erosion rates are plotted as a function of exposure time in Fig. 9. The results for the two collimators located at 25° were within 30% of one another, ranging from 11 to 15 μm/chr, and the rate decreased to ~ 3 μm/chr at 40°. The erosion rates were clearly insensitive to exposure time at each position. The uncertainties of sputter yield of quartz under xenon bombardment preclude converting these measurements to beam current densities. However, by assuming that the ion energies were constant across these angles the ratio of the current densities should equal the ratio of the erosion rates, indicating a factor of four decrease in current density between 25° and 40°. The current density measurements in Fig.5, obtained using the FMT, yield a current density of 0.025 A/m² at 25°, resulting in an estimated current density of 0.006 A/m² at 40°.

Tantalum target erosion measurements plotted as a function of angle from the ion beam axis are shown in Fig. 10. From these measurements, beam current densities were calculated using the sputter yield of tantalum under xenon bombardment, the atomic density of tantalum, the total exposure time (867 hrs), and assuming negligible charge-exchange current depletion from the beam. A sputter yield of 1.4 tantalum atoms per incident 1100 eV xenon ion was obtained by curve-fitting the measurements of Carter et al.¹⁷ and Roth et al.¹⁸ For the facility pressure of 1.3x10⁻⁴ Pa, charge-exchange should reduce the current density by less than 10%, well within the uncertainties of the sputter yield. Results of a comparison between the current densities calculated in this manner and those obtained by scaling the FMT ion beam current density measurements to the 9.4 m axial distance are shown in Fig. 11. The FMT results were scaled using an inverse z-squared dependence. The agreement between the two results indicates that the differences between the EMT and FMT beam profiles are minor.

Results from the QCMs and witness plates placed beneath the thruster showed that the sputtered material backflux resulted in an average deposition rate of 10 Å/hr. Mass gain measurements from the witness plates were converted to deposition rates assuming the

flux was pure iron from the facility walls. Results from the two QCMs were identical and showed no time dependence after the first 50 hours of thruster operation in both test segments.

Conclusions

Preliminary measurements of near and far-field ion current density distributions, doubly to singly charged ion current density ratios, and erosion and contamination were made for 30-cm ion engines in order to validate the diagnostics required for spacecraft integration assessments. Measurements were made for a Functional Model Thruster (FMT) and an Engineering Model Thruster (EMT). The measurements showed that the EMT had a beam flatness parameter of 0.47, near that of ion thrusters of similar design. The two dimensional far-field measurements showed that over 95% of the FMT ion beam is enclosed within a 22° half-angle, and that the thrust vector moved by less than 0.3° during throttling from 2.3 to 0.5 kW. The doubly to singly charged ion current ratio for the EMT ranged from 15% at 2.3 kW down to 5% at 0.5 kW. Erosion and contamination measurements showed that for angles greater than ~ 40° with respect to the thruster axis samples on the facility walls were subject to net deposition of eroded facility wall material. Collimated quartz samples, which were not impacted by deposition of eroded facility material, showed that the quartz erosion rate decreased from between 11 and 15 μm/chr to ~ 3 μm/chr as the angle with respect to the thruster axis increased from 25° to 40°. These erosion rates were not time dependent to first order. Facility sputtering resulting from ion beam impingement resulted in a backflux rate of ~10¹⁰ Å/hr at the ion thruster in the large VF 5 test facility.

Acknowledgements

The authors wish to thank John Naglowsky, Gene Pleban, Eli Green, George Jacynycz, Fred Jent, Bob Roman, Erhard Hartman, John Miller, Keith Johnson, Rob Butler, and Kevin Blake. We are also grateful to John Brophy for the use of the JPL ExB probe and to Jim Sovey for help with sputter yield estimates.

References

¹Bennett, G., et al., "Thrusting Toward Application: An Overview of NASA's Electric Propulsion Program," AIAA Paper 94-4136, Proceedings of the 29th Intersociety Energy Conversion Engineering Conference, Aug. 1994, pp. 743 - 743.

²Byers, D.C., "Electron Bombardment Thruster Field and Particle Interfaces," Journal of Spacecraft and Rockets, Vol., 16, No. 5., Sept. - Oct. 1979, pp. 289 - 301.

³Danilowicz, R.L., Rawlin, V.K., Banks, B.A., and Wintucky, E.G., "Measurement of Beam Divergence of 30-Centimeter Dished Grids," AIAA Paper 73-1051, Oct. 1973.

⁴Takegahara, H., et al., "Beam Characteristics Evaluation of ETS-VI Xenon Ion Thruster," IEPC Paper 93-235, Proceedings of the 23rd International Electric Propulsion Conference, Vol. 3, Sept. 1993, pp. 2166-2174.

⁵Groh, K.H., Fahrenbach, P., and Loeb, H.W., "Recent Ion Thruster Developments at Giessen University, IEPC Paper 93-105, Proceedings of the 23rd International Electric Propulsion Conference, Vol. 2, Sept. 1993, pp. 964 - 970.

⁶Sovey, J.S., "Improved Ion Containment Using a Ring-Cusp Ion Thruster," NASA TM-82990, AIAA Paper 82-1928, J. Spacecraft and Rockets, Vol. 21, No. 5, Sept. - Oct. 1984, pp. 488-495.

⁷Carruth, M.R., "A Review of Studies on Ion Thruster Beam and Charge-Exchange Plasmas," AIAA Paper 82-1944, Nov. 1982.

⁸Carruth, M.R., ed., "Experimental and Analytical Evaluation of Ion Thruster/Spacecraft Interactions," NASA CR-163975, January 1981.

⁹Sellen, J., et al., "Solar Electric Propulsion Instrument/Subsystems Interaction Study," NASA CR-114732, March 1973.

¹⁰Sovey, J. S. and Rawlin, V.K., "Characterization of In-Flight Performance of Ion Propulsion Systems," AIAA Paper 93-2217, June 1993; See also NASA TM 106283.

¹¹Patterson, M.J., Haag, T.W., and Hovan, S.A., "Performance of the NASA 30-cm Ion Thruster," IEPC Paper 93-108, Proceedings of the 23rd International Electric Propulsion Conference, Vol. 2, Sept. 1993, pp. 980 - 1014.

¹²Grisnik, S.P., and Parkes, J.E., "A Large High Vacuum, High Pumping Speed Space Simulation Chamber for Electric Propulsion," IEPC Paper 93-151, Proceedings of the 23rd International Electric Propulsion Conference, Vol. 2, Sept. 1993, pp. 1383 - 1390; See also NASA TM 106453.

¹³Smirnov, B.M. and Chibisov, M.I., "Resonance Charge Transfer in Inert Gases," Soviet Physics - Technical Physics, Vol. 10, No. 1, July 1965, pp. 88 - 92.

¹⁴Patterson, M.J., et al., "2.3 kW Ion Thruster Wear Test," AIAA Paper 95-2516, July 1995.

¹⁵Randolph, T., Pencil, E., and Manzella, D., "Far-Field Contamination and Sputtering of the Stationary Plasma Thruster," AIAA Paper 94-2855, June 1994.

¹⁶Beattie, J.R., Williams, J.D., and Robson, R.R., "Flight Qualification of an 18-mN Xenon Ion Thruster," IEPC Paper 93-106, Proceedings of the

23rd International Electric Propulsion Conference, Vol. 1, Sept. 1993, pp. 971 - 978.

¹⁷Carter, G. and Armour, D.G., "The Interaction of Low Energy Ion Beams with Surfaces," Thin Solid Films, 80 (1981) pp. 13 - 29.

¹⁸Roth, J., Bohdanský, J., and Ottenberger, W., "Data on Low Energy Light Ion Sputtering," IPP 9/26, Max-Planck-Institute für Plasmaphysik, Garching bei München, May 1979.

Thruster Power, kW	Beam Current, A	Facility Pressure, Torr	Beam Current corrected for charge exchange	Integrated Beam Current measured using probes
2.3	1.77	1.22×10^{-6}	1.70	1.71
1.5	0.98	9.8×10^{-7}	0.94	0.98
0.5	0.50	8.5×10^{-7}	0.48	0.53
2.3	1.72	9×10^{-6}	1.24	1.39

Table 1 - Beam currents compared to values obtained by integrating two dimensional probe measurements for FMT thruster at 3 power levels and two facility pressures in VF 5.

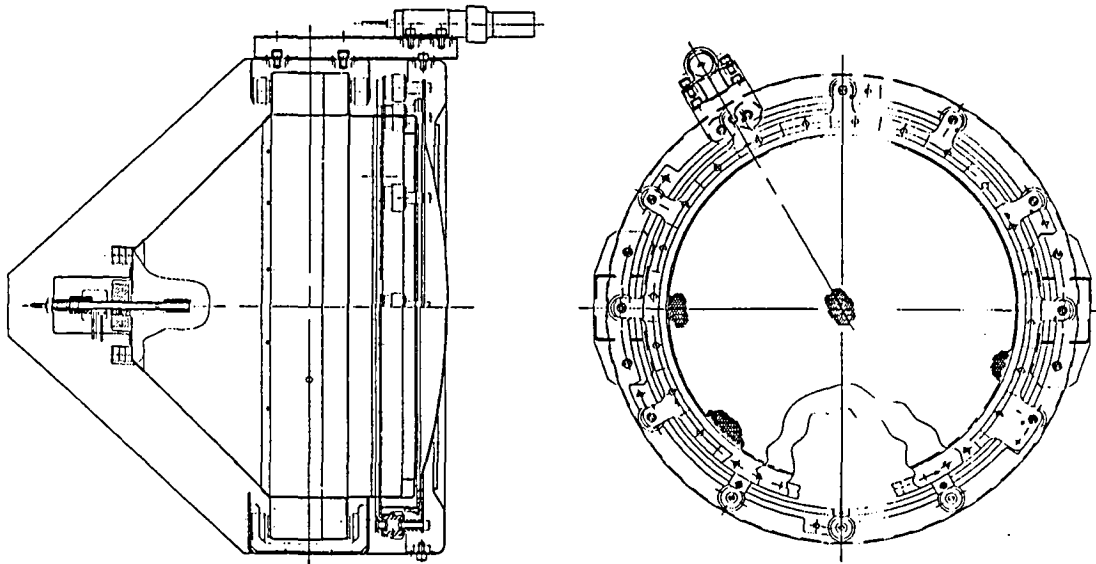


Fig. 1 - Engineering Model Thruster for NSTAR.

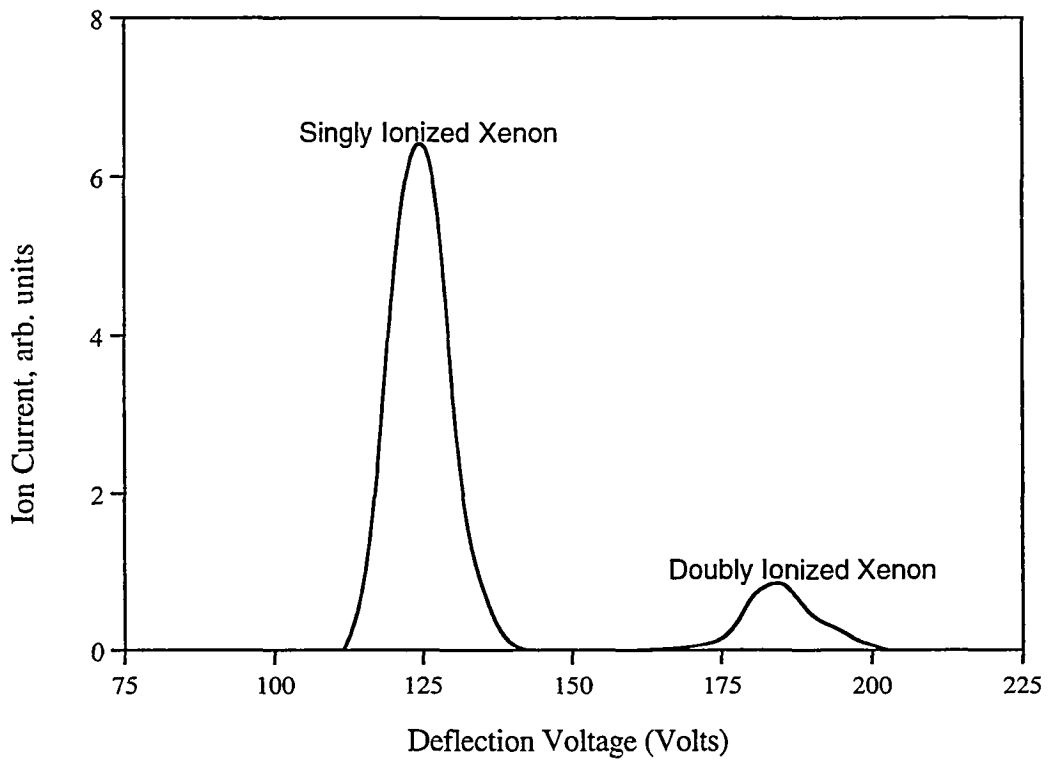


Fig 2 - Singly and doubly charged ion current peaks on centerline with EMT operating at 2.3 kW.

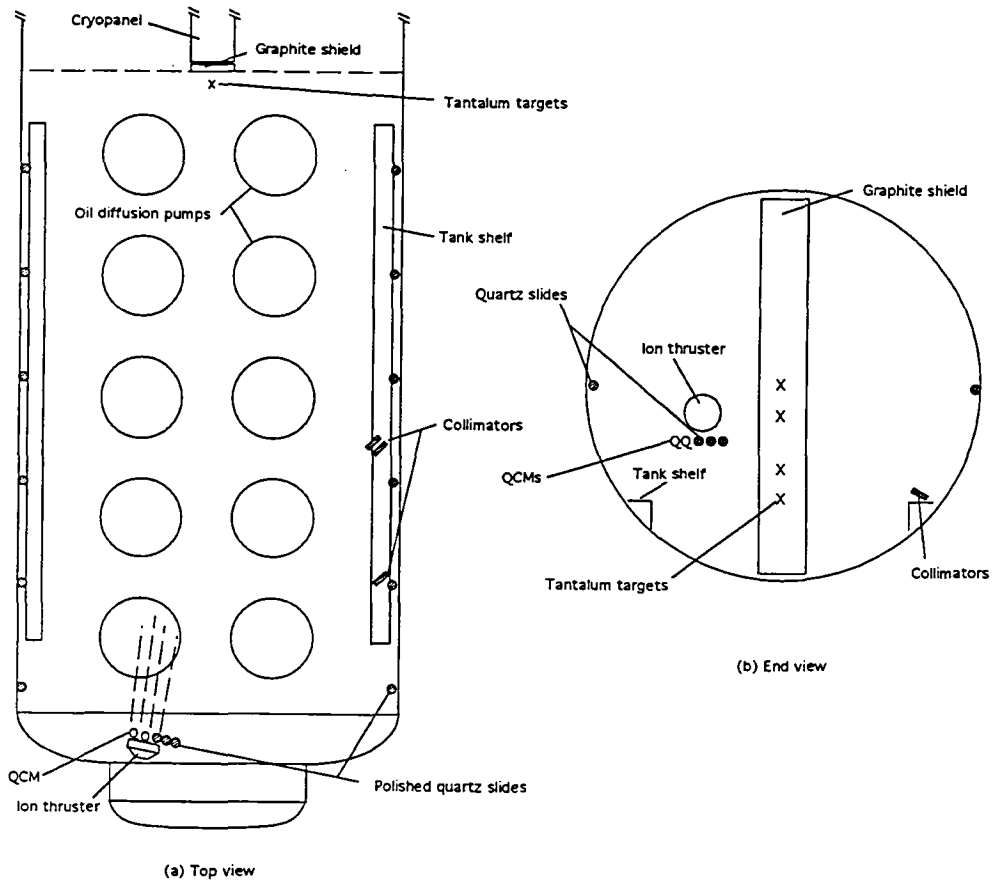


Fig. 3 - Location of contamination and sputtering sensors in the test facility.

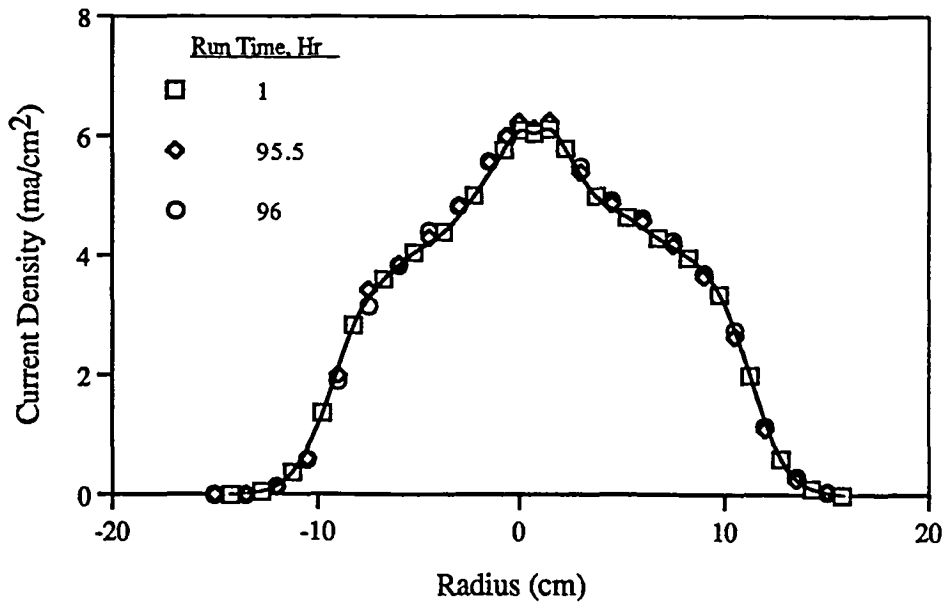
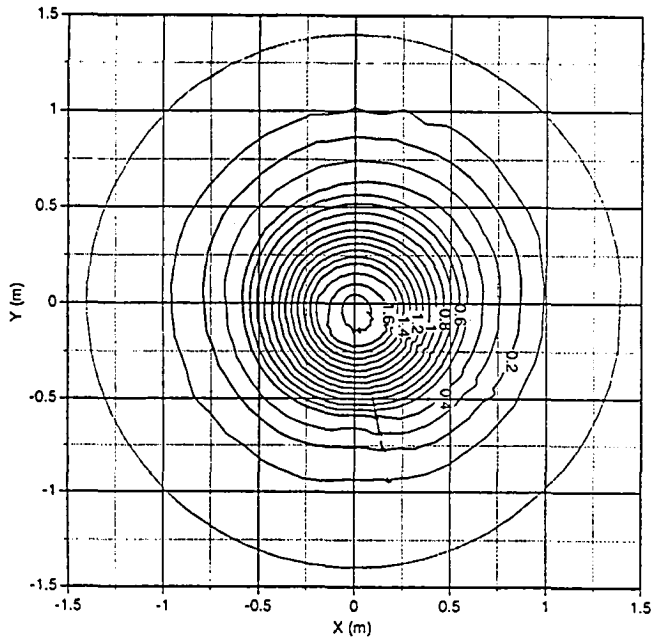
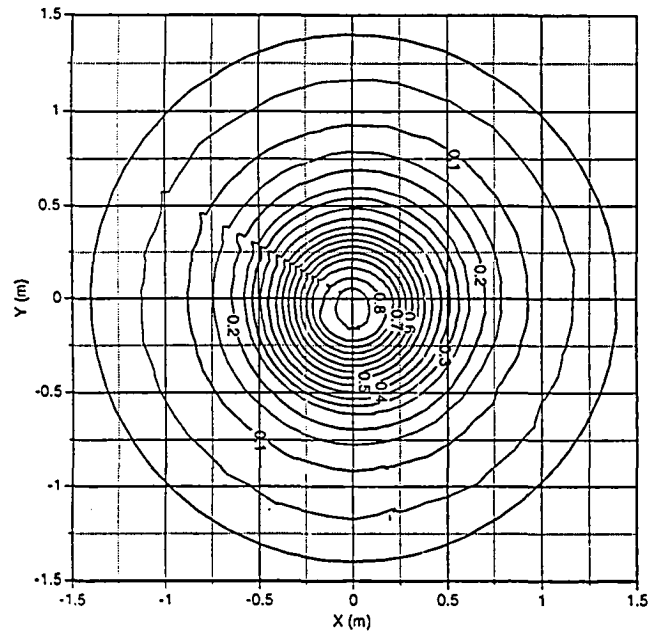


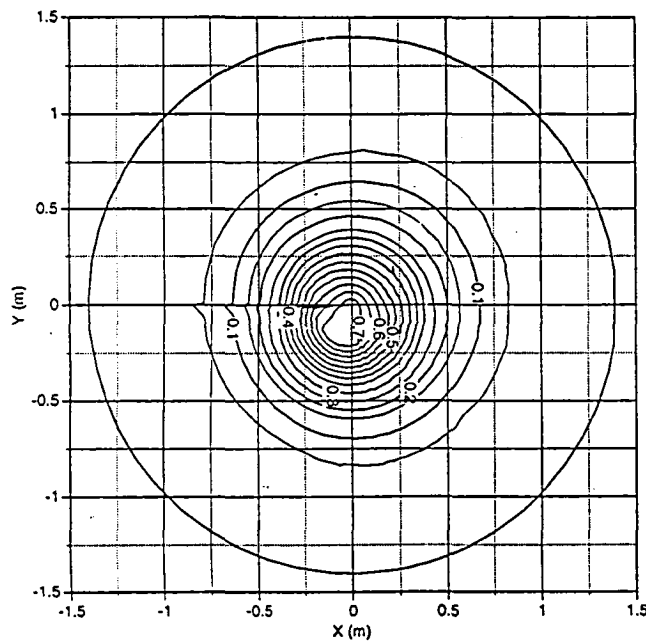
Fig. 4 - Near field ion current density for the EMT thruster at 2.3 kW.



(a) 2.3 kW, 1.77 A Beam



(b) 1.5 kW, 0.98 A Beam



(c) 0.5 kW, 0.50 A Beam

Fig. 5 - Current density (A/m^2) contour plots for the FMT thruster operating at 2.3, 1.5, and 0.5 kW.

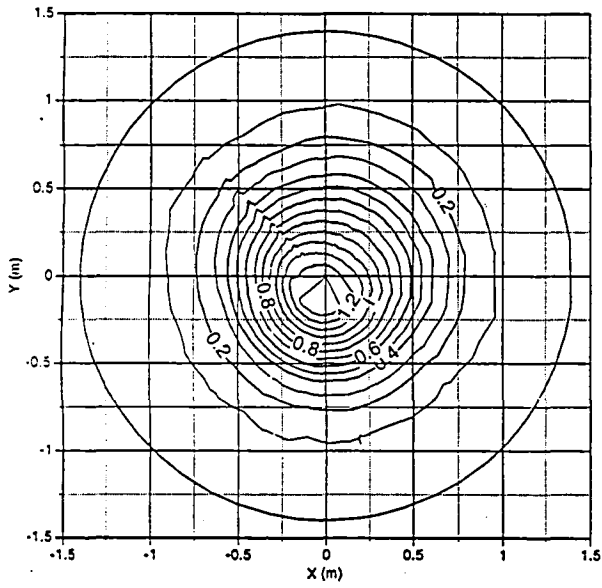


Fig. 6 - Current density contour (A/m^2) plot for the FMT thruster operating at 2.3 kW at a high facility pressure of 9×10^{-6} T.

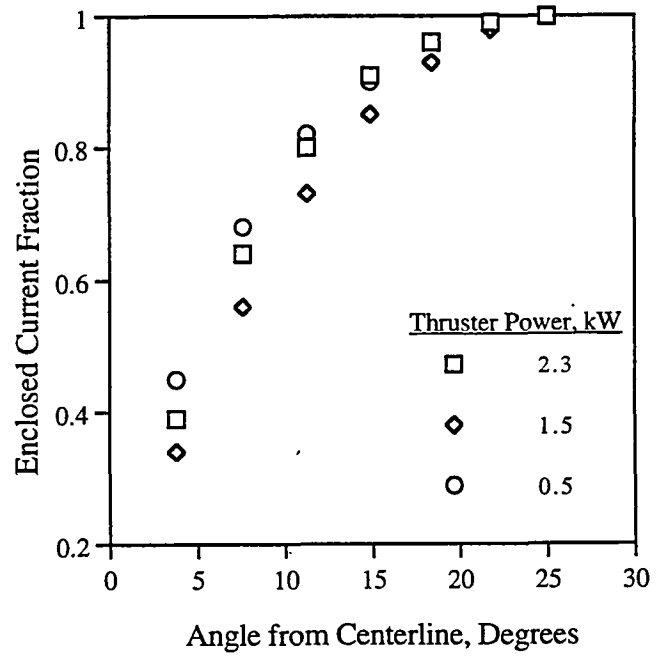


Fig. 7 - Enclosed current fraction vs. angle from beam centerline for the FMT at three power levels.

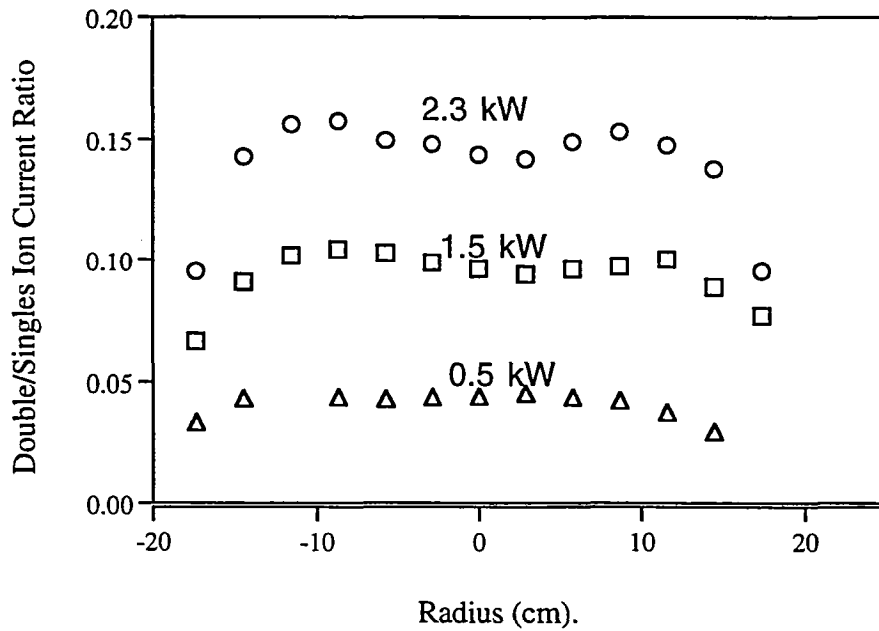


Fig. 8 - Ratio of doubly charged to singly charged ion current densities for EMT with the screen grid tied to cathode common.

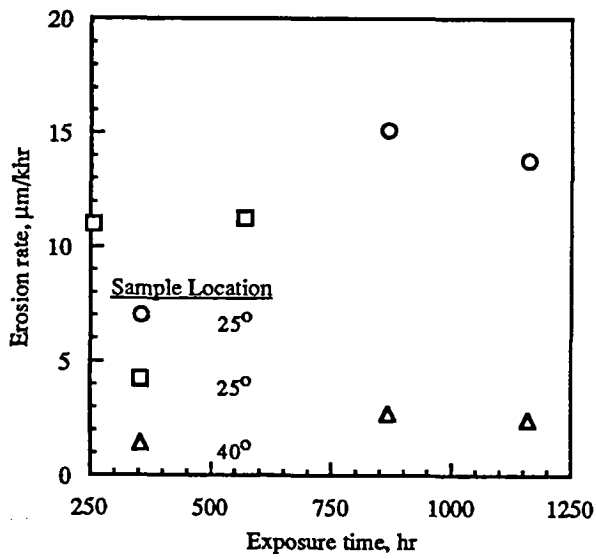


Fig. 9 - Erosion rates of collimated samples for four exposure times at two angles from the thruster axis.

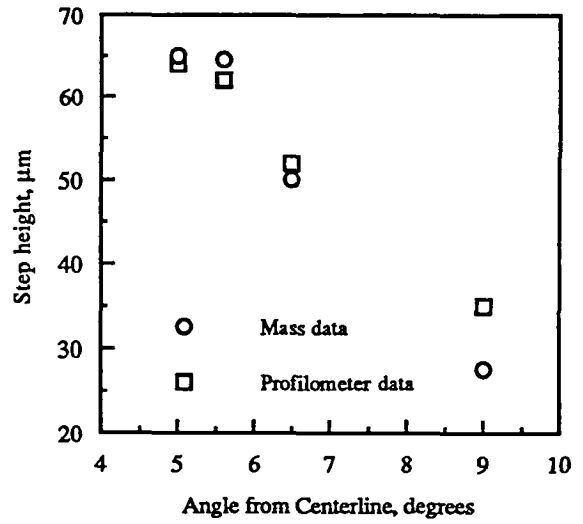


Fig. 10 - Erosion step height for tantalum targets 9.4 m from the EMT after 867 hour test segment.

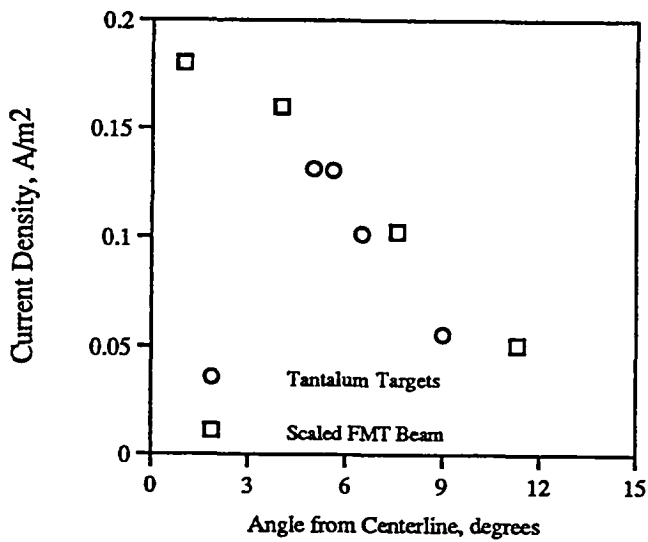


Fig. 11 - Beam current densities calculated from the tantalum target erosion data and the FMT beam current measurements.

REPORT DOCUMENTATION PAGE

Form Approved
OMB No. 0704-0188

Public reporting burden for this collection of information is estimated to average 1 hour per response, including the time for reviewing instructions, searching existing data sources, gathering and maintaining the data needed, and completing and reviewing the collection of information. Send comments regarding this burden estimate or any other aspect of this collection of information, including suggestions for reducing this burden, to Washington Headquarters Services, Directorate for Information Operations and Reports, 1215 Jefferson Davis Highway, Suite 1204, Arlington, VA 22202-4302, and to the Office of Management and Budget, Paperwork Reduction Project (0704-0188), Washington, DC 20503.

1. AGENCY USE ONLY (Leave blank)	2. REPORT DATE <p style="text-align: center;">September 1995</p>	3. REPORT TYPE AND DATES COVERED <p style="text-align: center;">Technical Memorandum</p>	
4. TITLE AND SUBTITLE <p style="text-align: center;">NSTAR Ion Thruster Plume Impacts Assessments</p>		5. FUNDING NUMBERS <p style="text-align: center;">WU-242-70-02</p>	
6. AUTHOR(S) <p style="text-align: center;">Roger M. Myers, Eric J. Pencil, Vincent K. Rawlin, Michael Kussmaul, and Katesha Oden</p>			
7. PERFORMING ORGANIZATION NAME(S) AND ADDRESS(ES) <p style="text-align: center;">National Aeronautics and Space Administration Lewis Research Center Cleveland, Ohio 44135-3191</p>		8. PERFORMING ORGANIZATION REPORT NUMBER <p style="text-align: center;">E-9898</p>	
9. SPONSORING/MONITORING AGENCY NAME(S) AND ADDRESS(ES) <p style="text-align: center;">National Aeronautics and Space Administration Washington, D.C. 20546-0001</p>		10. SPONSORING/MONITORING AGENCY REPORT NUMBER <p style="text-align: center;">NASA TM-107052</p>	
11. SUPPLEMENTARY NOTES Prepared for the 31st Joint Propulsion Conference and Exhibit cosponsored by AIAA, ASME, SAE, and ASEE, San Diego, California, July 10-12, 1995. Roger M. Myers and Michael Kussmaul, NYMA, Inc., 2001 Aerospace Parkway, Brook Park, Ohio 44142 (work funded by NASA Contract NAS3-27186); Eric J. Pencil and Vincent K. Rawlin, NASA Lewis Research Center, Katesha Oden, Tennessee State University, Nashville, Tennessee 37209. Responsible person, Eric J. Pencil, organization code 5330, (216) 977-7463.			
12a. DISTRIBUTION/AVAILABILITY STATEMENT <p style="text-align: center;">Unclassified - Unlimited Subject Category 20</p> <p style="text-align: center;">This publication is available from the NASA Center for Aerospace Information, (301) 621-0390.</p>		12b. DISTRIBUTION CODE	
13. ABSTRACT (Maximum 200 words) <p>Tests were performed to establish 30-cm ion thruster plume impacts, including plume characterizations via near and far-field ion current measurements, contamination, and sputtering assessments. Current density measurements show that 95% of the beam was enclosed within a 22° half-angle and that the thrust vector shifted by less than 0.3° during throttling from 2.3 to 0.5 kW. The beam flatness parameter was found to be 0.47, and the ratio of doubly charged to singly charged ion current density decreased from 15% at 2.3 kW to 5% at 0.5kW. Quartz sample erosion measurements showed that the samples eroded at a rate of between 11 and 13 μm/hr at 25° from the thruster axis, and that the rate dropped by a factor of four at 40°. Good agreement was obtained between extrapolated current densities and those calculated from tantalum target erosion measurements. Quartz crystal microbalance and witness plate measurements showed that ion beam sputtering of the tank resulted in a facility material backflux rate of ~10 Å/hr in a large space simulation chamber.</p>			
14. SUBJECT TERMS <p style="text-align: center;">Electric propulsion; Spacecraft integration</p>		15. NUMBER OF PAGES <p style="text-align: center;">13</p>	
		16. PRICE CODE <p style="text-align: center;">A03</p>	
17. SECURITY CLASSIFICATION OF REPORT <p style="text-align: center;">Unclassified</p>	18. SECURITY CLASSIFICATION OF THIS PAGE <p style="text-align: center;">Unclassified</p>	19. SECURITY CLASSIFICATION OF ABSTRACT <p style="text-align: center;">Unclassified</p>	20. LIMITATION OF ABSTRACT